Quality Enhancement of Gamma Camera SPECT Images Via the Taguchi-Based Optimization of Their Minimum Detectable Difference And a V-Shaped Slit Gauge

Ching-Hsiu Ke
Central Taiwan University of Science and Technology
Wan-Ju Liu
Taichung Tzu Chi General Hospital: Taichung Tzu Chi Hospital
Bing-Ru Peng
Taichung Armed Forces General Hospital
Lung-Fa Pan
Taichung Armed Forces General Hospital
Lung-Kwang Pan (lkpan@ctust.edu.tw)
CTUST: Central Taiwan University of Sciences and Technology https://orcid.org/0000-0002-9485-4722

Original research

Keywords: SPECT, gamma camera, Taguchi optimization, Tc-99m

Posted Date: October 28th, 2021

DOI: https://doi.org/10.21203/rs.3.rs-961592/v1

Quality enhancement of gamma camera SPECT images via the Taguchi-based optimization of their minimum detectable difference and a V-shaped slit gauge

Ching-Hsiu Ke[1,2], Wan-Ju Liu[1,3], Bing-Ru Peng[1,4], Lung-Fa Pan[1,5*], Lung-Kwang Pan[1 *]

These two co-authors equally contributed as corresponding authors

* Lung-Kwang Pan, email: lkpan@ctust.edu.tw

* Lung-Fa Pan, email: lung-fa@803.org.tw

Declarations:

Authors' contributions:

All authors participated in the concept of the paper. LK Pan wrote the manuscript. LF Pan contributed to the paper by correcting and reorganising the layout. WJ Liu and CH Ke did the experiment setup and data analysis. BR Peng obtained quantitive data and assessed image quality. All authors read and approved the final manuscript.

Funding:

The Ministry of Science and Technology of the Republic of China (contract No. MOST 110-2221-E-166-001) and the Central Taiwan University of Science and Technology (contract No. CTU109-P-105)

Availability of data and materials:

The datasets used and/or analysed during the current study are available from the corresponding author on reasonable request.

Ethics approval and consent to participate:

The study was approved by the Buddhist Dalin Tuzchi Hospital under IRB No. B11002019. All patients provided written informed consent.

Consent for publication:

All patients provided written informed consent.

Competing interests:

The authors declare that they have no conflict of interest

Author details:

1. Department of Medical Imaging and Radiological Science, Central Taiwan University of Science and Technology, Takun, Taichung 406, Taiwan, ROC. 2. Department of Optometry, Central Taiwan University of Science and Technology, Takun, Taichung 406, Taiwan, ROC. 3. Department of Nuclear Medicine, Taichung Tzu Chi Hospital, Buddhist Tzu Chi Medical Foundation, Taiwan, ROC. 4. Department of Radiology, Taichung Armed Forces General Hospital, Taichung 411, Taiwan; ROC. 5. Department of Cardiology, Taichung Armed Forces General Hospital, Taichung 411, Taiwan; ROC.

ABSTRACT

Background: This study optimized the minimum detectable difference (MDD) of gamma camera SPECT images via the Taguchi analysis and an indigenous V-shaped slit gauge. The latter was customized to satisfy the Taguchi analysis′ quantitative requirements.

Methods: The slit gauge MDD quantification of derived SPECT images was based on a pair of overlapped-peak profiles obtained from a tangent slice of the V-shaped slit with two adjacent peaks. Using the revised Student′s t-test with a multiplied constant, 1.96, the MDD was defined as the minimum distance between two peak centers, which deviation was large enough to ensure a 95% confidence level of their separation. In total, eighteen combinations of six gamma camera scanned factors (A-F), namely (A) collimator, (B) detector to target distance, (C) total counts, (D) acquired energy width, (E) Matrix size, and (F) zoom of collected ROI with each of two or three levels were organized into 18 groups to collect the slit gauge images according to Taguchi L_{18} orthogonal array. Next, three well-trained radiologists ranked the scanned gauge images to derive the fish-bone-plot of signal-to-noise ratio (S/N, dB) and correlated ANOVA.

Results: The quantified MDD was proposed to verify the optimal suggestion of gamma camera scanned protocol, and obtained the MDD as 8.44, 7.88, and 7.40 mm for the 2nd group of the original L_{18}, conventional, and optimal presets, respectively.

Conclusions: The optimal preset of gamma camera was achieved according to Taguchi analysis. The MDD-based approach was found more beneficial in evaluating the spatial resolution than the line pair/cm approach in routine quality control in this study.

Keywords: SPECT, gamma camera, Taguchi optimization, Tc-99m

1. Introduction

The minimum detectable difference (MDD) of gamma camera SPECT (Single Photon Emission Computed Tomography) images was optimized through the Taguchi analysis and an indigenous V-shaped slit gauge in this study. Bone scan is common examination in the nuclear medicine of most hospitals because it can provide bountiful information of local blood flow and bone metabolic activity. It is a fast-screening tool for whole-body bone cancer metastasis [1, 2] and is more efficient in tracking the preliminary syndrome from increased blood flow or osteogenetic activity enhancement than routine X-ray diagnosis because the latter requires the bone calcium changing by over ±35-50% for causing the apparent lesion [3, 4]. Meanwhile, bones are one of the most common sites for metastases of all cancers, thus, an optimal preset of regular bone scan protocol can greatly help in examining the carcinoma in early stage from radiological viewpoint [5-7].

Therefore, researchers have developed various techniques to enhance the quality of scanned images of gamma camera by their pre/post-processing. Oumar and Ercelebi [8] used an indigenous phantom to evaluate the integral and differential uniformity of gamma camera images for the quality control. The phantom was customized by many slits or holes with various sizes and the infused radioactive solution was Tc-99m. Alternatively, Robert et al. [9] utilized a commercial phantom to optimize the spatial resolution of imaging by a joint application of a practical figure of merit (FOM) and theoretical simulation. Hruska et al. [10] and Dickerscheid [11] also used multiple-hole phantoms of various sizes to optimize the image quality by justifying the contrast-to-noise ratio and collimator.

In contrast to the above approaches, this study optimizes the gamma camera SPECT images

by the Taguchi analysis, which proved to be efficient in radiological field. Yeh et al. [12] first adopted this technique in nuclear medicine examination with a semi-quantitative phantom to optimize the imaging quality, while Kittipayak et al. [13] applied this method to a simple self-developed phantom to optimize the imaging quality of head and neck diagnosis in routine nuclear examination. The Taguchi analysis became a mature and robust tool providing efficient and confident solution with practical verification. Thus, the optimal protocol of gamma camera from Taguchi's recommendation is always strongly valid with bountiful numerical proof in reality. Meanwhile, the quantified gauge is also essential in verifying the optimization, whereas the minimum detectable difference (MDD) is preferable for representing the spatial resolution.

2. Materials and Methods

2.1 Taguchi analysis

Optimization of high-quality characteristic systems is commonly performed by the Taguchi analysis, which organizes unique orthogonal arrays and assesses large factor contributions by processing a limited set of measured data. The optimal combination of six factors controlling the gamma camera scanned image quality was derived, and less relevant factors were tuned out. The statistical analysis of variance (ANOVA) was conducted to evaluate the main influencing factors of the aim variable. The signal-to-noise (S/N) and ANOVA analyses were comprehensively combined and run to provide the optimal gamma camera scan protocol factor settings [14,15].

2.2 Orthogonal arrays

In contrast to other optimization methods, the Taguchi analysis furnishes either an optimal value of a single assigned factor from a limited practical data array or detects the main influencing factors controlling the aim variable behavior. The six factors of the gamma camera scan protocol included the (A) collimator, (B) Detector to target distance (DTD), (C) total counts (TC), (D)

acquired energy width (EW), (E) Matrix size of acquired image, and (F) Zoom for specific ROI. Thus, a total of 486 (2×3×3×3×3×3) combinations was concerned, because each of these factors could be defined into two or three levels. Adopting the Taguchi analysis, the measurements were arranged into only eighteen groups, which were collected to acquire outcomes in the same confidence level as that from some conventional, thorough optimal processes [16]. Table 1 presents a standard L_{18} ($2^1 \times 3^5$) orthogonal array recommended by Taguchi; the digits in every column imply the levels, or practical arrangements, for the particular factors (A-F). Table 2 depicts the six factors (A-F) as (A) collimator, (B) DTD (C) TC, (D) EW, (E) Matrix, and (F) Zoom.

2.3 ANOVA Analysis of Variance

A practical loss function η, which could easily be converted to signal-to-noise (S/N) ratio, was introduced by Taguchi to quantify the performance qualities. A high S/N value corresponded to a high-quality characteristic and the maximization produced the optimal factor settings [16]. Using the loss function, the gamma camera scan image quality can be determined from the specific V-shaped slit gauge by adopting various gamma camera scan protocols as follows:

$$\eta_i = -10\, log\left[\left(\frac{1}{Y(i)_{avg}}\right)^2 + \left(\frac{stdev}{Y(i)_{avg}}\right)^2\right] \quad (1)$$

where η_i is the loss function (S/N unit: *dB*) of the i^{th} group. A larger value of η is preferable in this case, since the rank of the scanned V-shaped slit gauge image is defined via the "higher-is-better" principle. Thus, eighteen is the highest ranking in this work. The following set of equations is used:

$$SS_{Total} = \left[\sum_{i=1}^{n}\sum_{j=1}^{r} y_{ij}^2\right] - n \times r \times \overline{\overline{y}}^2 \quad (2)$$

$$SS_{Factor} = \frac{n \times r}{L} \sum_{k=1}^{L} (\overline{y_k} - \overline{\overline{y}})^2 \quad (3)$$

$$SS_{error} = SS_{total} - \sum_{i=1}^{n} SS_{Factor_i} \quad (4)$$

$$DoF_{Total} = n \times r - 1;\ DoF_{Factor} = L - 1;\ DoF_{error} = n \times (r - 1) \quad (5)$$

In Eq.(2), SS_{Total} is all squared variances' sum, $y_{ij,}$ is the image ranked grade for the i^{th} group in the j^{th} trial, and *r* is the total number of each group's trial repeats. This study adopted *r*= 9, which corresponded to three rounds of ranking of the same slit gauge image by three radiologists (3×3=9). In Eqs.(1) and (2), $\overline{\overline{y}}$ is the average of all ranked values of the instant slit gauge image, which theoretical value is 9.5. In Eq.(2), SS_{Factor} is the sum of respective squared values corresponding to a particular factor, while $\overline{y_k}$ is the average ranked value assigned to that factor. *L* and *n* are the number of levels assigned to the factor and all groups (L=2 or 3 and *n* =18), respectively. SS_{error} is the sum of squared random errors only. In Eq.(5), F_{factor} is the practical index of the *F-test*. When assessing each individual factor, the following dependence was used

$$F_{factor} = \frac{SS_{factor}}{DoF_{factor}} / \frac{SS_{error}}{DoF_{error}} \quad (6)$$

where DoF_i is the number of degrees of freedom of each factor (equal to 1 or 2 in this study). Finally, the random error is equal to the deviation of nine ranked grades assigned in three rounds by the three radiologists, yielding DoF_{error} =18×(9-1)= 144 in (Eq. 5) [17].

2.4 The V-shaped slit gauge and Gamma camera

The V-shaped slit gauge was specially designed to facilitate the revised t-test analysis. The zigzag array of the slit with a continuous change of slit depth provided the respective gamma-ray

image under scanning and, thus, the converted data matrix of derived SPECT could be evaluated for calculating the revised t-test index. Moreover, the data profile of SPECT could be judged channel-by-channel to ensure that two adjacent peaks satisfied a 95% confidence level according to definition of revised t-test after the conversion from the original gamma-ray imaging. Thus, the MDD could be quantified as precise as to 0.1 mm rather than providing an approximate value within a 0.3-0.6 mm range of the intrinsic spatial resolution for referring in reality [18].

Figure 1(A) shows the precise designation chart of this unique PMMA V-shaped slit gauge (200×200×18 mm^3). The V-shaped slit maintained the shallowest depth (2.0 mm) at the top right V-shape, then went deeper along the slit to the bottom one (4.8 mm). The fixed slit width of 1.0 mm was designed along the pathway. It contained either seven or eight V-shaped triangles on the left or right bottom edges, respectively. The bottom edge width dropped in the following order: right bottom (167-134= 33 mm), left bottom (150.5-119.5= 31 mm), right top bottom (20-15=5 mm), and left top bottom (24.5-17.5=7 mm). Accordingly, for any vertical tangent line cutting across both sides of the triangle, one could easily assess its edge distance by the proportional principle, judging from its bottom edge and the distance to the triangular vertex, insofar as the height of each triangle was fixed at 170 mm (185-15= 170 mm). Thus, the MDD of SPECT was defined by the quantification of the tangent line from the digitalized image after the SPECT image conversion from the real gamma camera scans.

In contrast to the majority of commercially available planar line phantoms and test patterns, which implied a lead bar to create a hot slit/cold background [19], the V-shaped slit gauge provided the hot-line image with the intense-to-feeble gradation and the wide-to-narrow triangular shape for the imaging quality judgment. As shown in Figure 1(B), a 7.4 MBq Tc-99m radioactive solution was diluted to 11 c.c. and dyed with blue ink for easier identification. Then, it was thoroughly injected into the phantom deepest part to let the solution fill in along the V-shaped pathway for the

gamma camera scanning. As seen in Figure 1(C), the radioactive V-shaped slit gauge was placed between two water containers, each filled at a 15 cm-deep level by water mixed with 0.925MBq Tc-99m. Then, the gauge was scanned by the gamma camera (GE Infinia Hawkeye 4 SPECT/CT), as depicted in Figure 1(D). In addition, the clinical spine-to-soft tissue ratio in routine abdomen scan was $37.8 \pm 9.5/9.7 \pm 9.5$(counts/pixel) $=3.9 \pm 3.2$ under a 95% confidence level from ten randomly chosen patients in hospital, whereas the radioactive intensity of preset V-shaped slit gauge to the background (the sum of two water containers) was $41.8 \pm 3.9/11.5 \pm 0.9$ (counts/pixel) $=3.6 \pm 0.4$, indicating an appropriate ratio preset in this study.

2.5 V-shaped slit gauge ranking

A high detectable difference between V-shaped slits is an intrinsic feature of gamma camera scan images with a strong contrast and fine resolution combination, allowing one to distinguish the fuzzy section. The available images were ranked by a trio of seasoned radiologists according to the double-blind criteria, minimizing the human factor-induced bias of the final ranking [20]. The "higher-is-better" S/N definition via Eq.(1) was applied to the ranked grade. To quantify the actual MDD values for the derived SPECT images, the MATLAB default function (/imread) converted them into a digital matrix as in [21].

2.6 MDD and revised Student's t-test analysis

The spatial resolution of gamma camera SPECT images can be evaluated by the individual FWHM parameter (i.e., full width at half maximum) of the specific peak using a single peak profile. Alternatively, this study used tangent slices of the V-shaped slit with two adjacent peaks to quantify the minimum detectable difference (MDD) using two overlapped-peak profiles. The Student's t-test formula was revised by multiplying it to a constant factor of 1.96, indicating that the two peak

centers deviated far enough from each other to ensure a 95% confidence level of their separation [22]:

$$|X_1 - X_2| \geq 1.96 \times \sqrt{\left(\frac{FWHM_1}{2}\right)^2 + \left(\frac{FWHM_2}{2}\right)^2} \qquad (7)$$

where X_1 and X_2 are the centers of peaks 1 and 2, respectively, while FWHM is the full width at half maximum of the specific peak. The MDD evaluation for two adjacent peaks was performed via the unique V-shaped slit by gradually changing the valley edge of two peaks, yielding its edge width's quantitative estimate.

Due to its high distinguishable ability in analyzing the spine structure, low values of MDD are favorable in the gamma camera scan images. Consider the following cases for the two adjacent peaks in Figure 2:(A) they were identified as wholly separated; (B) they barely passed the student's t-test evaluation; (C), the distance is too small for differentiating them. Different from the reports based on the qualitative and human factor-biased judgments of radiologists, the above ones were obtained via quantitative criteria of passing or failing the revised student's t-test, being entirely supported by the calculation results. Thus, the quantified MDD can provide an auxiliary tool in justifying the performance of gamma camera scanned images rather than radiologists' visual ranking, although manual judgement is still essential in the preliminary sorting stage of Taguchi analysis.

3. Results

3.1 Data analysis

Figure 3 shows the eighteen original images of gamma camera scans according to the Taguchi's eighteen groups of factor combinations. The ideal images should have a strong black-

and-white contrast ratio and a sharp edge along the V-shaped slit. In most of them, peaks from 1 to 6 could be easily distinguished, in contrast to peaks 7 and 8. Thus, the precision of peak nine (cf. Fig. 1(A), 5 mm of the bottom edge) is beyond the analytical ability of routine gamma camera whereas, peak eight (cf. Fig. 1(A), 9 mm of the bottom edge) is the critical element, which will be explained in the following discussion. Table 3 summarizes the original ranked grade, average, standard deviation (stdev), and S/Ns values corresponding to the three radiologists in three discrete rounds (Equation 1). The stdev values were assessed the ranked grade y_i in each group, being further rearranged for each factor, together with the average and S/N values. Thus, the factor B (DTD) effect on the quality of gamma camera scan images at various levels (1, 2, or 3) was reflected by the average grades of groups (1, 2, 3, 10, 11, 12), (4, 5, 6, 13, 14, 15) or (7, 8, 9, 16, 17, 18), as shown in Tables 1 and 2. The dependences linking average, stdev, and S/N values with each of six factors of the gamma camera scan protocol were visualized as fish-bone-plots in Figure 4. According to Table 3, the highest average, stdev and S/N values (namely, 16.6, 0.9 and 21.88 were observed in Group 2. Accordingly, the recommended preset of six factors for the gamma camera scanned imaging system comprised (A) LEHR collimator, (B) 5 cm DTD, (C) 150k TC, (D) 16% EW, (E) Matrix size 256×256, and (F) 1.28 ZOOM, which combination maintained the highest S/N value for each factor (cf. Fig. 4, S/N(dB)).

3.2 ANOVA analysis results

The ranking of the dominant factors controlling gamma camera scan image quality was further verified by the F-test via Eq. (6). Table 4 summarizes the confidence levels of factors assigned to the virtue of the gamma camera scans. Since highly contributing factors were recognized as dominant ones, factor A (collimator) with a 38.5%, contribution, factor B (DTD) with 41.0%, and factor F (Zoom) with 4.0% were found to the most crucial for the V-shaped slit gauge imaging

quality. However, since four out of six factors were significant and exhibited a medium correlation among factors (cf. Tab. 4), none of these six factors could be adjusted individually to ensure a high rank.

4. Discussion

4.1 Verifying the Taguchi recommendation by quantified MDD

Taguchi analysis helps efficiently in optimizing the gamma camera scanned imaging in the first stage according to the unique eighteen orthogonal array. Then, the quantified MDD is provided to further verify the optimization process. The calculated MDD can precisely quantify the performance of scanned image than radiologists' visual judgement in the second stage, although the professional judgement on the basis of double-blinded principle is a quite reliable tool. Figure 5 demonstrates the three derived SPECT and practical images from gamma camera scans:(A) group 2 with the highest S/N of the 18 original Taguchi's eighteen groups, (B) a conventional preset, and (C) the combination of the highest S/N values for each specific factor (cf. Fig. 4, beyond the original eighteen groups. As clearly depicted in cases (A) and (B), angles 8 and 9 on the right edge are mixed together (cf. Fig. 1(A) top right edge width was 5 mm.) Noteworthy is that the acquired images from practical gamma camera were mirror-reflected, whereas in case (C), the angle 9 could be barely identified. Nevertheless, by the definition of MDD, none of three cases satisfies the criteria of MDD gaining a 95% confidence level from angle 8 and 7 (cf. Fig. 1(A), bottom edge is 29-20=9 mm). Thus, we focus on the MDD between angles 7 and 6 (bottom edge is 42-29=13 mm) because the slit of this triangle had a deeper depth of 2.8 mm than that between angles 7 and 8 of 2.4 mm (cf. Fig. 1(A)). A deeper depth can deposit a comparatively higher contrast media solution than shallow one and yield a brighter image for calculation. Table 5 shows the correlated calculation of MDD between angles 6 and 7 of three cases in this study. The channel number, as

adopted in Eq.(7), was obtained from the SPECT for the specific case (cf. Fig. 5). Apparently, the recommend second group in the original L_{18} array had the largest MDD since it could not well separate angles 7 and 8, whereas the optimal one had the smallest MDD of 7.40 mm, and the conventional one had a medium MDD of 7.88 mm. In addition, the three different protocols of gamma camera were rearranged and listed in Table 6. As clearly demonstrated, factors had to be compromised altogether, before minimizing the MDD in reality. The quantified MDD provided a solid numerical information to help radiologists in routine quality control rather than visual inspection according to commercial phantoms or line pair gauges.

4.2 Quantified MDD advantages of the line/pair approach

The quantified MDD can also be converted to the line pair/cm (lp/cm) form for justifying the gamma camera scanned imaging quality optimization, although these two approaches have been developed according to different scenarios. The MDD was proposed to identify the minimum distance between two peaks within a 95% confidence level, whereas the lp/cm concept concerns two bright and dark lines. Furthermore, the MDD can be theoretically reduced by the confidence level from 95% to 68%, which will exclude the multiplication factor of 1.96 in Eq. 7. Figure 6 presents a diagram, which shows the difference between MDD and lp/cm. The former can be interpreted as having a similar width to one line pair. Thus, the number of lp/cm approximately equals to 10mm/MDD, although MDD provides a more precise information. Thus, the roughly estimated lp/cm values are 1.2, 1.3, and 1.4 for the second, conventional and the optimal groups, respectively. Nevertheless, the lp/cm approach offers only quantized numbers, while MDD uses two adjacent peaks from the real gamma camera scanned images.

4.3 Clinical verification of gamma camera optimal preset

To further validate the gamma camera optimal preset, the latter's scanned image was compared to that with the conventional preset as shown in Figure 7. As clearly depicted, the optimal preset

yielded clearer images with greater contrast than the conventional one. Specifically, the shadow of the ribs and pelvis could be clearly identified, and the sacroiliac joint could also be delineated in the optimal preset's image. The clinical procedures had been accomplished between June and December, 2021 under IRB No. B11002019 approved by the Buddhist Dalin Tuzchi Hospital. The imaging system optimization improved the quality of gamma camera images, ensuring more reliable clinical examination results.

5. Conclusions

The minimum detectable difference (MDD) of gamma camera SPECT images was optimized through the Taguchi analysis and an indigenous V-shaped slit gauge in this study. The eighteen groups of factor combinations were organized according to Taguchi unique orthogonal array and ranked by three seasoned radiologists to derive the signal-to-noise ratio and construct the fish-bone plots of average, stdev, and S/N values. The quantified MDD values were 8.44, 7.88, and 7.40 mm for the second group of the original L_{18}, conventional, and the optimal presets, respectively. The MDD-based approach was found more beneficial in evaluating the spatial resolution than the line pair/cm approach in routine quality control, although these two could be mutually converted through a simple equation. The optimal preset of gamma camera was verified by the clinical examination, providing a sharp delineation of zones of interest.

6. Acknowledgments

The authors highly appreciate the financial support of this study by the Ministry of Science and Technology of the Republic of China (contract No. MOST 110-2221-E-166-001) and the Central Taiwan University of Science and Technology (contract No. CTU109-P-105)

References

1. Yu CC, Ting CY, Yang MH, Chan HP: **Comparison of irregular flux viewer system with BONENAVI version for identification of Tc-99m MDP whole body bone scan metastasis images.** Journal of X-ray Sci. and Tech 2021, **29**(4):617-633.
2. Pawar SU, Dharmalingum A, Bhatt BM, Shetye SS, Ghorpade MK. **Role of Tc-99m MDP bone scan in evaluation of osteoid osteoma at varied locations.** Intl J Res in Med Sci 2018, **6**(8):2711-2716.
3. Das D, Das M. **Vegetation Ecology of Coastal belt of Khejuri area of Purba Medinipur District with special reference to Hijli coast, West Bengal, India.** IOSR J. of Pharmacy 2014, **4**(2):56-77.
4. Archi A, Prafulla J, Nilendu P, Sneha S, Venkatesh R. **Rare splenic metastasis of renal cell carcinoma detected on 99m Tc-MDP bone scan.** Indian Journal of Nuclear Medicine 2014, 29(1):60-61.
5. Araz M, Aras G, Kucuk ON. **The role of 18F–NaF PET/CT in metastatic bone disease.** J of Bone Oncology 2015, **4**:92-97.
6. Iagaru A, Mittra E, Dick DW, Gambhir SS. **Prospective Evaluation of ^{99m}Tc MDP Scintigraphy, ^{18}F NaF PET/CT, and ^{18}F FDG PET/CT for Detection of Skeletal Metastases.** Molecular Imaging and Biology 2012, **14**:252-259.
7. Zhang L, He Q, Zhou T, Zhang B, Li W, Peng H, Zhong X, Ma L, Zhang R. **Accurate characterization of ^{99m}Tc-MDP uptake in extraosseous neoplasm mimicking bone metastasis on whole-body bone scan: contribution of SPECT/CT.** BMC Medical Imaging

2019, 19:44. https://doi.org/10.1186/s12880-019-0345-1

8. Oumar AA, Ercelebi E. **Assessment of an in-house phantom for the quality control of a clinical gamma camera.** Journal of X-Ray Science and Technology 2020, **28**(3):461-470.
9. Robert C, Montemont G, Rebuffel V, Buvat I, Guerin L, Verger L. **Simulation-based evaluation and optimization of a new CdZnTe gamma-camera architecture (HiSens).** Phys. Med. Biol. 2010, **55**:2709-2726.
10. Hruska CB, Weinmann AL, O'Connor MK. **Proof of concept for low-dose molecular breast imaging with a dual-head CZT gamma camera. Part I. Evaluation in phantoms.** Med. Phys. 2012, **39**(6):3466-3475.
11. Dickerscheid D, Lavalaye J, Romijn L, Habraken J. **Contrast-noise-ratio (CNR) analysis and optimisation of breast-specific gamma imaging (BSGI) acquisition protocols.** EJNMMI Research 2013, 3:21. http://www.ejnmmires.com/content/3/1/21
12. Yeh DM, Chang PJ, Pan LK. **The optimum Ga-67-citrate gamma camera imaging quality factors as first calculated and shown by the Taguchi's analysis.** Hell J Nucl Med. 2013, **16**(1):25-32.
13. Kittipayak S, Pan LF, Chiang FT, Pan LK. **The Optimization of the Single Photon Emission Computed Tomography Image Quality via Taguchi Analysis: A Feasibility Study of a V-Shaped Phantom.** J. Medical Imaging and Health Informatics 2017, **7**(1):143-148.
14. Chen CY, Liu KC, Chen HH, Pan LK. **Optimizing the TLD-100 readout system for various radiotherapy beam doses using the Taguchi methodology.** Appl. Radi. and Isot. 2010, **68**(3):481-488.
15. Pan LK, Chou DS, Chang BD, **Optimization for solidification of low-level- radioactive resin using Taguchi analysis.** Waste Management 2001, **21**:762-772.
16. Roy RK, **A primer on the Taguchi method**, 2nd ed. Society of Manufacturing Engineering,

USA ISBN 13:978-0-87263-864-8

17. Yoo SK, Cotton SL, Sofotasios PC, Matthaiou M, Valkama M, Karagiannidis GK. **The Fisher–Snedecor F distribution: A simple and accurate composite fading model.** IEEE commu. Letter 2017, **21**(7):1661-1664.

18. Nakanishi K, Yamamoto S, Kataoka J. **Performance comparison of finely channeled LYSO- and GAGG-based Si-PM gamma cameras for high-resolution SPECT.** NIMA A 2017, **872**:107-111.

19. Noori-Asl M, Sadremomtaz A, Bitarafan-Rajabi A. **Evaluation of three scatter correction methods based on the estimation of photopeak scatter spectrum in SPECT imaging: A simulation study**. Physica Medica 2014, **30**:947-953.

20. Misra S, **Randomized double blind placebo control studies, the "Gold Standard" in intervention based studies**. Indian J Sex Transm Dis AIDS 2012, **33**(2):131-134.

21. MATLAB. **Matrix laboratory developed by MathWorks**. V7.0.1.24704 (R14), 2004. http://www.mathworks.com/products/matlab/whatsnew.html

22. Kenny DA, Mannetti L, Pierro A, Livi S, Kashy DA. **The statistical analysis of data from small groups.** J Personal Soc Psychol 2002, **83**(1):126-137.

Table1. The standard L_{18} ($2^1 \times 3^5$) Taguchi's orthogonal array; the numbers correspond to levels (or practical layouts) of the special factors (A-F).

Group	Factor					
	A	B	C	D	E	F
1	1	1	1	1	1	1
2	1	1	2	2	2	2
3	1	1	3	3	3	3
4	1	2	1	1	2	2
5	1	2	2	2	3	3
6	1	2	3	3	1	1
7	1	3	1	2	1	3
8	1	3	2	3	2	1
9	1	3	3	1	3	2
10	2	1	1	3	3	2
11	2	1	2	1	1	3
12	2	1	3	2	2	1
13	2	2	1	2	3	1
14	2	2	2	3	1	2
15	2	2	3	1	2	3
16	2	3	1	3	2	3
17	2	3	2	1	3	1
18	2	3	3	2	1	2

Table 2. The gamma camera scan protocol with six factors, each having two or three levels as suggested by the Taguchi L_{18} orthogonal array. Here, LEHR and LEGP are low-energy high-resolution and low-energy general-purpose, respectively.

Factor	Level 1	Level 2	Level 3
(A) collimator	LEHR	LEGP	
(B) detector to target distance (DTD)	5 cm	10 cm	15 cm
(C) Total counts (TT)	135k	150k	165k
(D) acquired energy width (EW)	16%	20%	24%
(E) Matrix size	128×128	256×256	512×512
(F) Zoom of ROI	1.00	1.28	1.50

Table 3. The estimates of three radiologists in three discrete rounds for the original ranked grade, average, standard deviation (stdev), and S/N values via Eq.(1). The stdev values were obtained from nine ranked grades, y_i, in each group.

Group	Radiologist-1			Radiologist-2			Radiologist-3			*Ave.*	*Sd*	*S/N*
1	16	18	18	11	17	14	18	15	18	16.1	2.4	15.78
2	18	17	17	16	16	16	15	17	17	16.6	0.9	21.88
3	13	16	16	18	13	18	12	18	14	15.3	2.4	15.42
4	12	14	11	17	15	17	13	16	14	14.3	2.1	15.72
5	11	12	14	15	7	12	8	13	12	11.6	2.6	12.35
6	15	15	15	13	18	15	16	12	15	14.9	1.7	17.59
7	6	5	3	8	8	7	3	9	8	6.3	2.2	8.25
8	8	9	12	12	14	10	14	10	9	10.9	2.2	13.06
9	9	8	8	9	11	9	9	8	7	8.7	1.1	15.24
10	10	10	9	10	6	11	7	7	11	9.0	1.9	12.55
11	14	11	10	14	9	8	10	11	10	10.8	2.0	13.50
12	17	13	13	7	12	13	17	14	16	13.6	3.1	12.42
13	7	6	7	6	10	5	11	6	3	6.8	2.4	8.21
14	5	4	4	4	5	6	6	4	5	4.8	0.8	11.29
15	4	7	5	5	4	4	4	5	6	4.9	1.1	10.54
16	1	2	1	1	2	1	5	1	2	1.8	1.3	0.69
17	3	3	6	3	3	3	2	3	4	3.3	1.1	6.94
18	2	1	2	2	1	2	1	2	1	1.6	0.5	2.77
Average										**9.5**	**1.8**	**11.90**

Table 4. The confidence levels of six factors under study related to the gamma camera scan protocol effectiveness. A factor is considered significant if its confidence level is no less than 99%.

Factor	SS	DOF	Contribution	Var	F	Probability	Confidence level	Significant
A	1694.91	1	38.5%	1694.9	463.42	0.0%	100.0%	Yes
B	1784.53	2	41.0%	892.3	243.96	0.0%	100.0%	Yes
C	17.20	2	0.4%	8.6	2.35	9.9%	90.1%	No
D	2.68	2	0.06%	1.3	0.37	69.4%	30.6%	No
E	55.46	2	1.4%	27.7	7.58	0.07%	99.9%	Yes
F	176.64	2	4.0%	88.3	24.15	0.0%	100.0%	Yes
Others	110.41	6	2.5%	18.4	5.03	0.01%	100.0%	Yes
Error	526.67	144	12.1%	3.7		S =1.91		
Total	4368.49	161	100%		*Note: At least 99% confidence level			

Table 5. The precise calculation of the revised Student's t-test for MDD. The channel number, as adopted in Eq.(7), was obtained for the of specific case of SPECT (cf. Fig. 5).

Channel no. of the derived SPECT	$\|X_1 - X_2\| \geq 1.96 \times \sqrt{\left(\frac{FWHM_1}{2}\right)^2 + \left(\frac{FWHM_2}{2}\right)^2}$
2nd group	$\|354 - 323\| \geq 1.96 \times \sqrt{\left(\frac{15}{2}\right)^2 + \left(\frac{16}{2}\right)^2}$ $\|31\| \geq 1.96 \times \sqrt{56.25 + 64}$ $31.0 \geq 21.5$
Conventional	$\|371 - 340\| \geq 1.96 \times \sqrt{\left(\frac{24}{2}\right)^2 + \left(\frac{8}{2}\right)^2}$ $\|31\| \geq 1.96 \times \sqrt{144 + 16}$ $31.0 \geq 24.8$
The Optimal	$\|375 - 342\| \geq 1.96 \times \sqrt{\left(\frac{21}{2}\right)^2 + \left(\frac{20}{2}\right)^2}$ $\|33\| \geq 1.96 \times \sqrt{110.25 + 100}$ $33.0 \geq 28.4$

Table 6. The MDD of a 2.8 mm-deep V-shaped slit derived for the second group's, conventional, and optimal factor settings of the gamma camera scan protocol.

Factor	2nd group	Conventional	Optimal
(A) Collimator	LEHR	LEHR	LEHR
(B) Det. to Target Distance	5cm	5cm	5cm
(C) Total Counts	150k	165k	150k
(D) Acquired Energy width	20%	16%	16%
(E) Matrix size	256×256	256×256	256×256
(F) Zoom	1.28	1.28	1.28
MDD	**8.44 mm**	**7.88 mm**	**7.40 mm**

Figure captions

Figure 1. (A) The precise designation chart of this unique PMMA V-shaped slit gauge (200×200×18 mm^3). The fixed slit width of 1.0 mm was designed along the pathway. (B) a 7.4 MBq Tc-99m radioactive solution was diluted to 11 c.c. and dyed with blue ink for easier identification inside the gauge, (C) the radioactive V-shaped slit gauge was placed between two water containers, each filled at a 15 cm-deep level by water mixed with 0.925MBq Tc-99m for scanning, (D) gamma camera GE Infinia Hawkeye 4 SPECT/CT in this study.

Figure 2. (A) two peaks can be identified as wholly separated, (B) two peaks barely passed the student's t-test evaluation, (C) the two peaks are too close to be differentiated.

Figure 3. Eighteen original scanned images from the gamma camera according to the Taguchi's eighteen factor combinations.

Figure 4. The fish-bone-plots of average, stdev, and S/N values versus six factors of the gamma camera scan protocol.

Figure 5. The three derived SPECT and original images from gamma camera scanned according to (A) group 2 of the original Taguchi's eighteen groups with the highest S/N value, (B) conventional preset, and (C) the combination of the highest S/N values for each specific factor.

Figure 6. The diagram shows the difference between MDD and line pair/cm results. The MDD can be interpreted as having a similar width to one line pair.

Figure 7. The optimal preset yielded clearer images with greater contrast than the conventional one. Specifically, the shadow of the ribs and pelvis could be clearly identified, and the sacroiliac joint could also be delineated from the optimal preset's image.

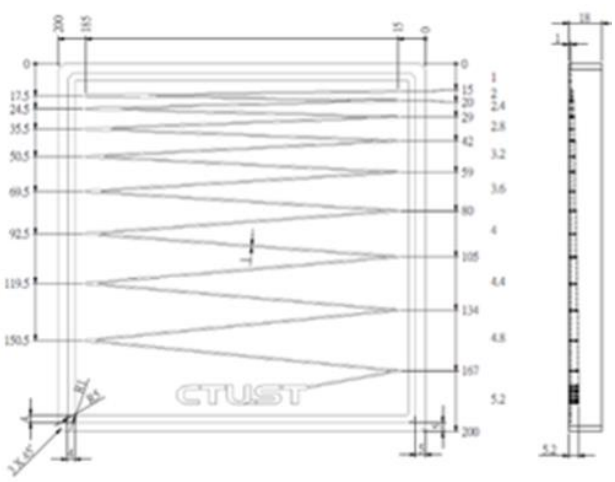

A

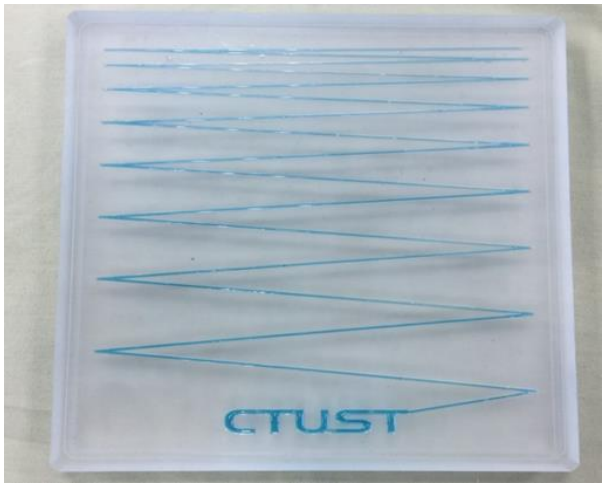

B

C

D

Fig. 1

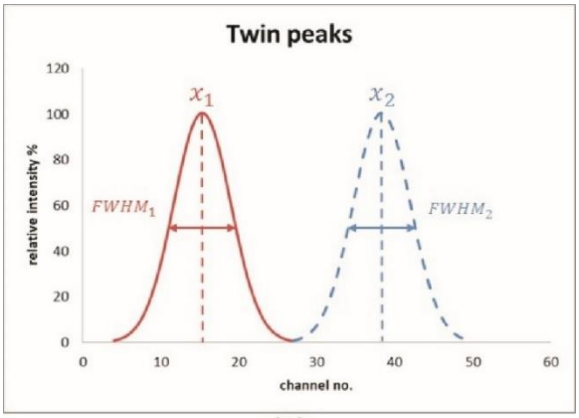
Twin peaks
relative intensity %
channel no.
x_1
x_2
$FWHM_1$
$FWHM_2$
0
20
40
60
80
100
120
0
10
20
30
40
50
60

(A)

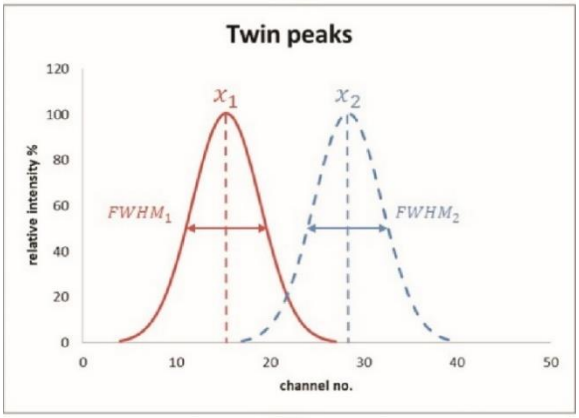
Twin peaks
relative intensity %
channel no.
x_1
x_2
$FWHM_1$
$FWHM_2$
0
20
40
60
80
100
120
0
10
20
30
40
50

(B)

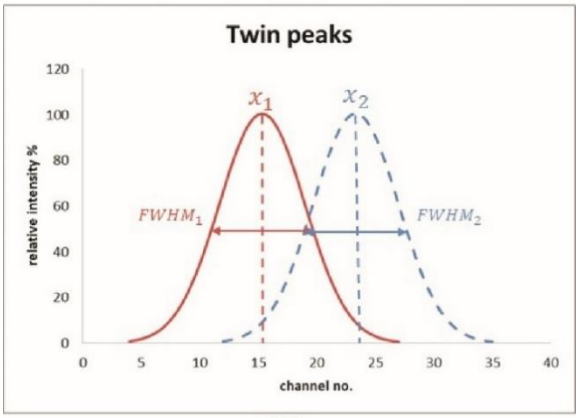
Twin peaks
relative intensity %
channel no.
x_1
x_2
$FWHM_1$
$FWHM_2$
0
20
40
60
80
100
120
0
5
10
15
20
25
30
35
40

(C)

Fig. 2

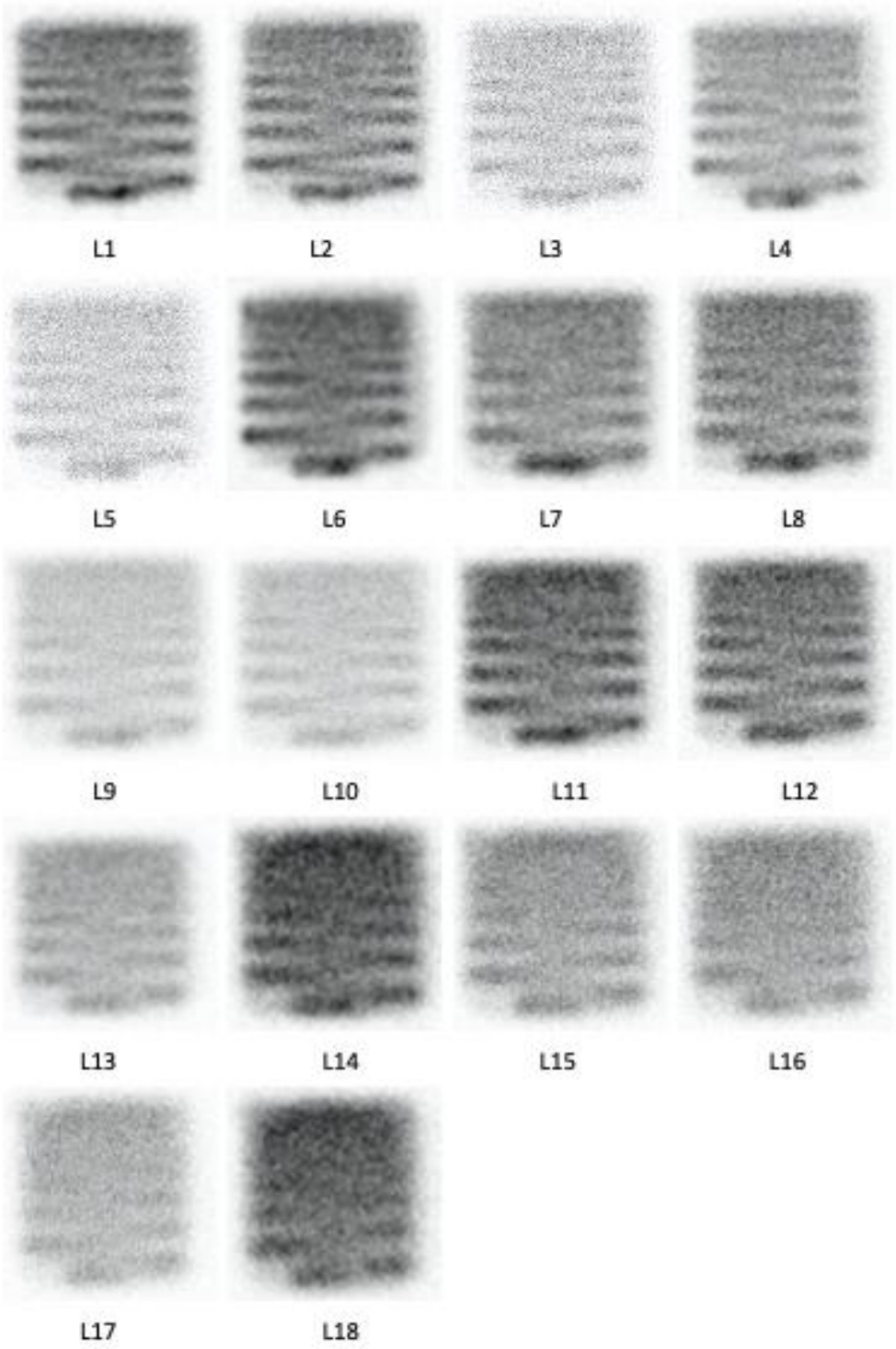

Fig. 3

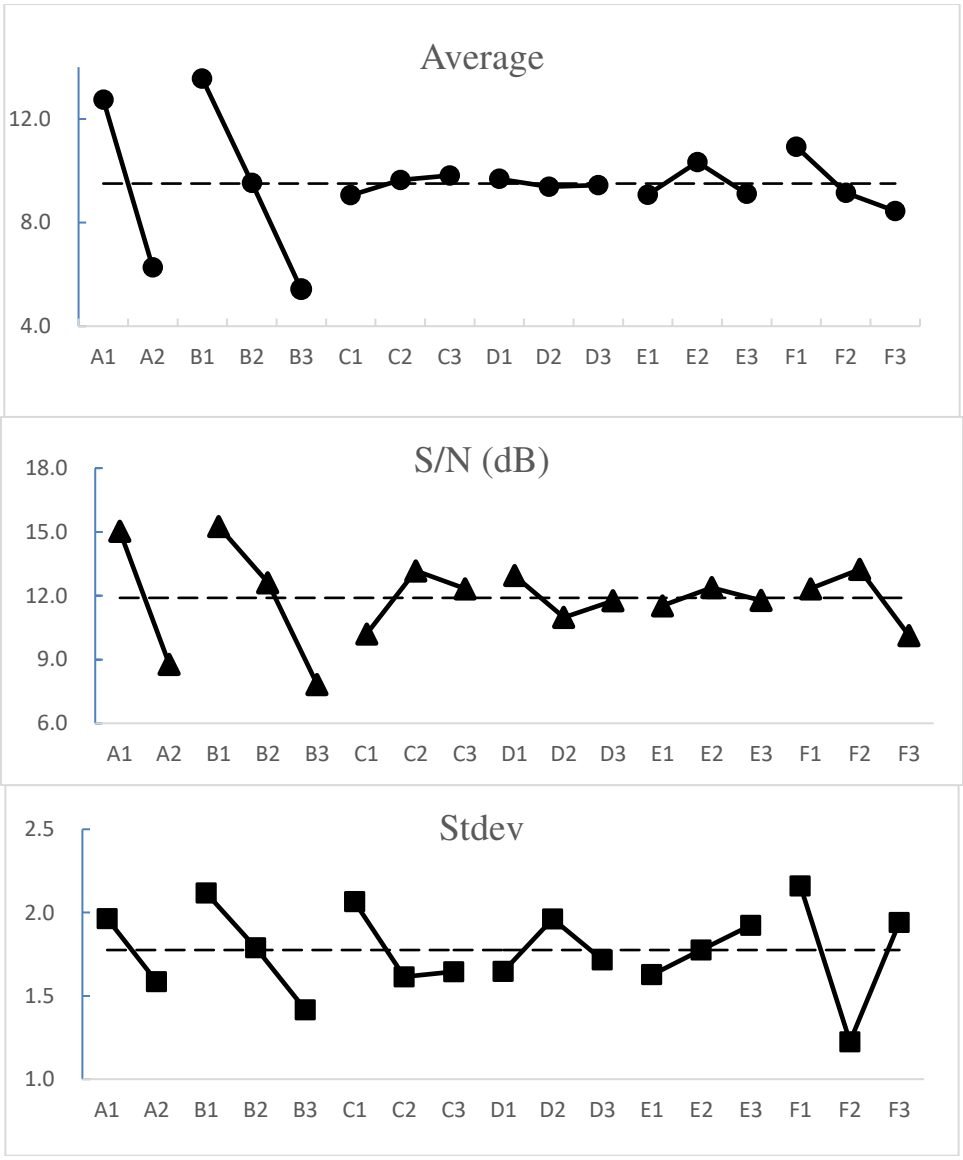
Average
12.0
8.0
4.0
A1 A2 B1 B2 B3 C1 C2 C3 D1 D2 D3 E1 E2 E3 F1 F2 F3
S/N (dB)
18.0
15.0
12.0
9.0
6.0
A1 A2 B1 B2 B3 C1 C2 C3 D1 D2 D3 E1 E2 E3 F1 F2 F3
Stdev
2.5
2.0
1.5
1.0
A1 A2 B1 B2 B3 C1 C2 C3 D1 D2 D3 E1 E2 E3 F1 F2 F3

Fig. 4

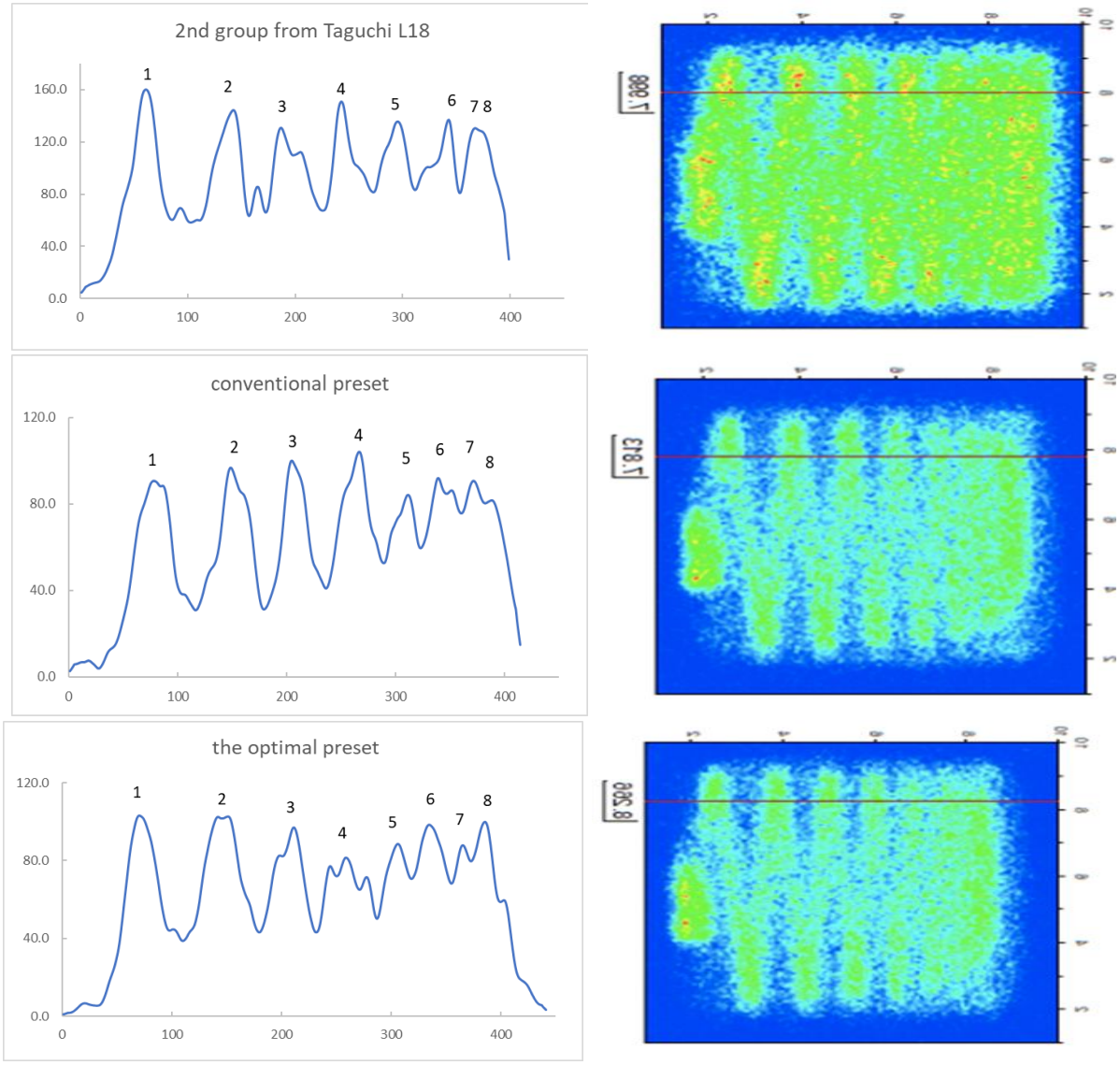
2nd group from Taguchi L18
160.0
120.0
80.0
40.0
0.0
0
100
200
300
400
1
2
3
4
5
6
7 8
conventional preset
120.0
80.0
40.0
0.0
0
100
200
300
400
1
2
3
4
5
6
7
8
the optimal preset
120.0
80.0
40.0
0.0
0
100
200
300
400
1
2
3
4
5
6
7
8

Fig. 5

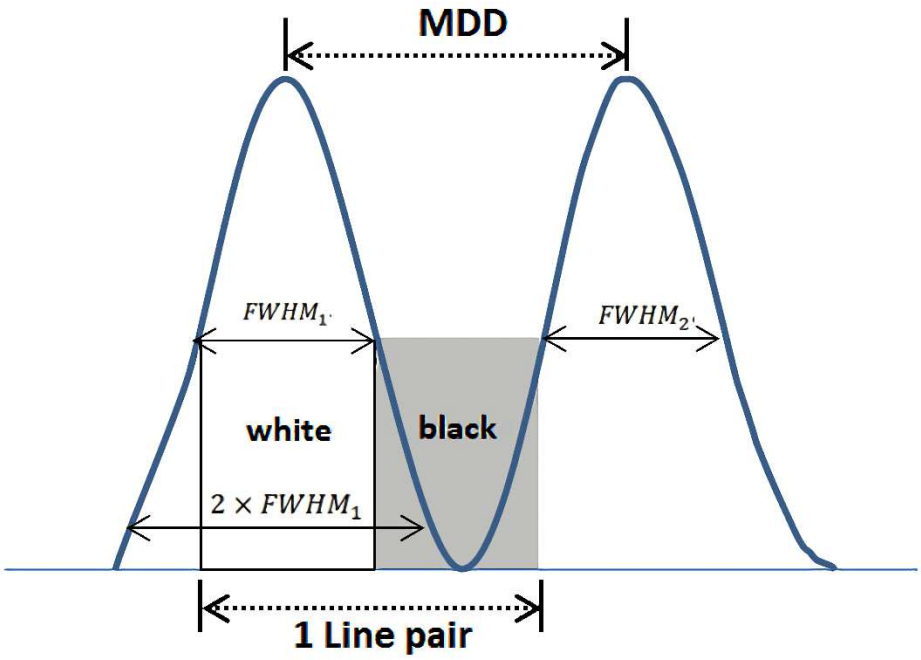

Fig. 6

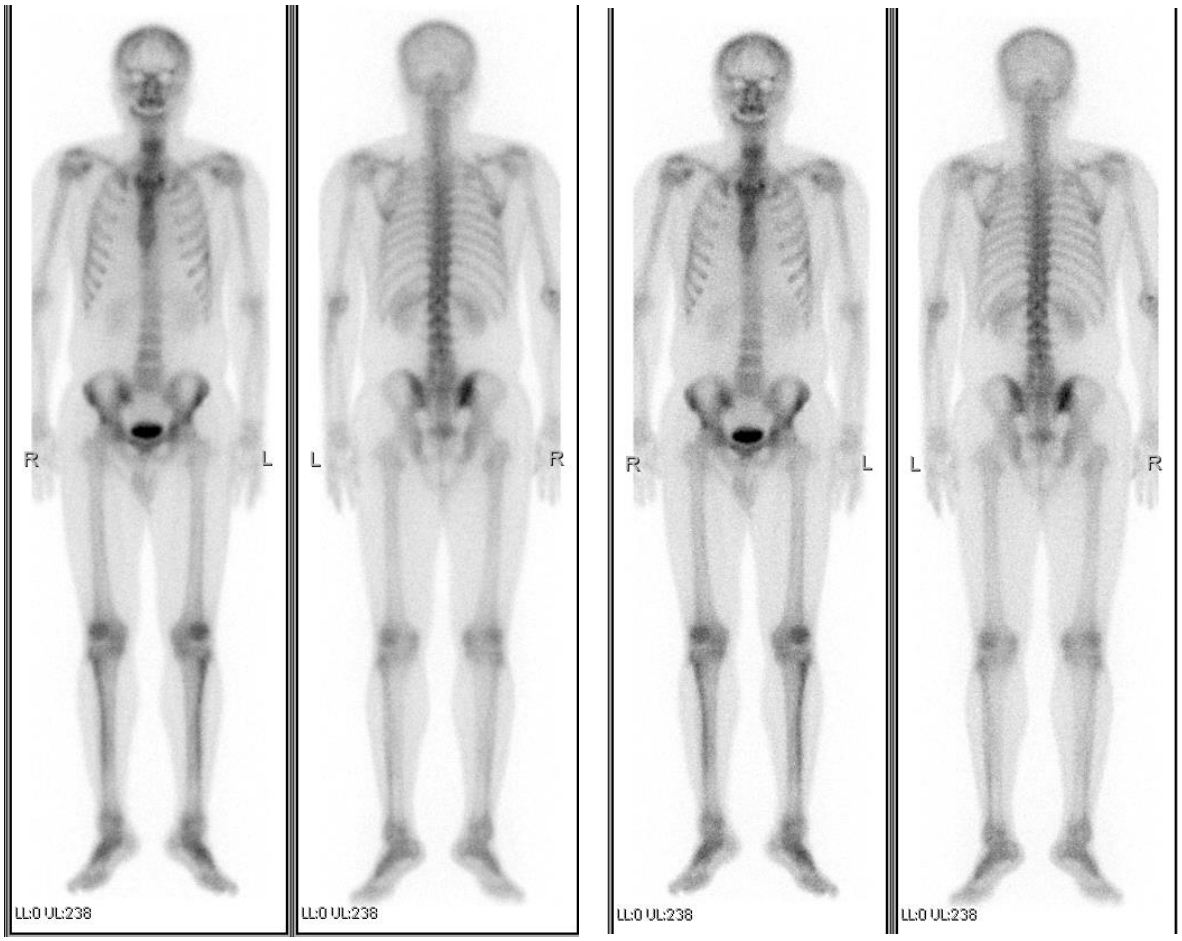

Conventional preset The optimal preset

Fig. 7